CHAPTER 4

PARTITIONING INTO OCTANOL

In all other sections of this book, we use the term K_p to represent the partition coefficient and K_d, the apparent partition coefficient. These terms were chosen to avoid symbol conflict when discussing permeability and diffusivity. Since this chapter and Chapter 5 are devoted primarily to partition coefficients, we will use the most common terminology: P for partition coefficients and D for apparent (pH-dependent) partition coefficients. [Other symbols for these parameters have been used in the literature, including P_{OW} (oil-water partition), K_{OW}, PC, and APC.]

Central to the Hansch analysis [17,98] is the use of $\log P$ or $\log D$ to predict biological activity. Much literature has been published about the measurement and applications of these parameters [17,23,24,57,98–100,224,225,243,245–265]. Two conferences have been dedicated to the topic [266,267]. Several studies [245,246,268] describe how to measure $\log P / \log D$: which techniques to use, what pitfalls to look out for, what lipid : water volumes to consider, the value of GLP—in other words, how to do it right. The structure of octanol became better understood [99,100]. Issues of water drag were investigated [247,248]. Partition solvents other than octanol ($CHCl_3$, various alkanes, PGDP, and 1,2–dichloroethane) were explored for the effect of their hydrogen bonding donor/acceptor properties [17,151,249,261,269]. Seiler's [250] concept of $\Delta \log P$ was further tested [251,252,257]. Methods to predict H-bond factors from two-dimensional structures were expanded [254–260]. Hydrogen bonding was prodded as ''the last mystery in drug design'' [253]. The concept of ''molecular chameleons,'' proposed by Testa and others, was applied to the study of intramolecular effects

in morphine glucuronide conformational-sensitive partitioning [151,262,263]. A case was made for the return of olive oil, as a model solvent in the prediction of partitioning into adipose tissue [264].

Today almost every practicing pharmaceutical scientist knows the difference between $\log P$ and $\log D$ [229,270–276]. Better understanding of the partitioning behavior of ampholytes and charged species emerged [277–291]. The concept of the micro-$\log P$ was formalized [224,243,273,275]. Rapid high-performance liquid chromatography (HPLC) methods for determining $\log P$ were fine-tuned [292–298]. Immobilized artificial membrane (IAM) chromatography [47,299–311], liposome chromatography [312–319], and capillary electrophoresis [320–322] evoked considerable interest. An accurate (compared to shake-flask) and fast (2 h) method using dialysis tubing to separate the aqueous phase from the octanol phase was reported [323]. Potentiometric methods of $\log P$ determination matured and achieved recognition [25,112,149–151,153,161,162,166,172,224,225,250,268,269, 275,324–363]. Some remarkable new insights were gained about the membrane interactions of charged amphiphilic species from the study of drug partitioning into liposomes (Chapter 5). The need for high-throughput measurements led to the scaling down of several techniques to the 96-well microtiter plate format [294].
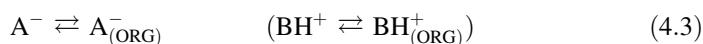
4.1 TETRAD OF EQUILIBRIA

The topic of drug partitioning between water and lipids concerns chemical equilibria. For a monoprotic weak acid (and base), the partitioning equilibria may be represented as
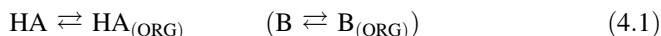
$$HA \rightleftarrows HA_{(ORG)} \qquad (B \rightleftarrows B_{(ORG)}) \tag{4.1}$$

As mentioned in Chapater 3, the law of mass action sets the concentration relations of the reactants and products. So, the equilibrium constants, termed the partition coefficients, are the quotients

$$P_{HA} = \frac{[HA_{(ORG)}]}{[HA]} \qquad \left(P_{B} = \frac{[B_{(ORG)}]}{[B]}\right) \tag{4.2}$$

where [HA] ([B]) is the free-acid (free-base) aqueous concentration, moles/liter aqueous solution, and the ORG-subscripted term is the concentration in the oil phase, moles/liter *of organic solvent* [347]. When the partition coefficient is determined directly, usually the aqueous concentration is determined analytically (UV or HPLC), and the oil-phase counterpart is inferred through mass balance [245]. Not only the neutral species, but the charged species can partition into the organic phase (such as octanol), although usually to a much lesser extent:

$$A^- \rightleftarrows A^-_{(ORG)} \qquad (BH^+ \rightleftarrows BH^+_{(ORG)}) \tag{4.3}$$

$$P_A = \frac{[A^-_{(ORG)}]}{[A^-]} \qquad \left(P_{BH} = \frac{[BH^+_{(ORG)}]}{[BH^+]}\right) \tag{4.4}$$
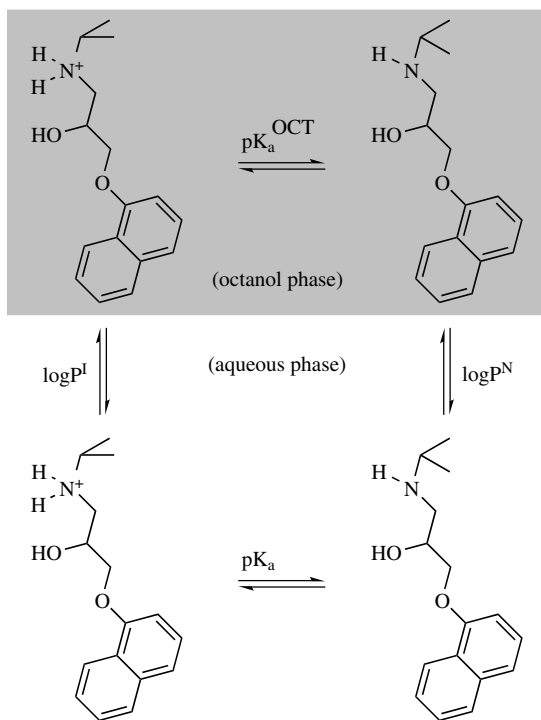
Figure 4.1   Octanol–water tetrad equilibria. [Avdeef, A., *Curr. Topics Med. Chem.*, **1**, 277–351 (2001). Reproduced with permission from Bentham Science Publishers, Ltd.]

To distinguish partition coefficients of neutral species from ionized species, the notation $\log P^N$ and $\log P^I$ may be used, respectively, or the symbol C or A may be used as a substitute for superscript I, denoting a cation or anion, respectively. [362].

It is convenient to summarize the various reactions in a box diagram, such as Fig. 4.1 [17,275,280], illustrated with the equilibria of the weak base, propranolol. In Fig. 4.1 is an equation labeled pK_a^{oct}. This constant refers to the octanol pK_a, a term first used by Scherrer [280]. When the concentrations of the uncharged and the charged species *in octanol* are equal, the *aqueous* pH at that point defines pK_a^{oct}, which is indicated for a weak acid as

$$HA_{(ORG)} \rightleftarrows A^-_{(ORG)} + H^+ \qquad K_a^{oct} = \frac{\left[A^-_{(ORG)}\right][H^+]}{\left[HA_{(ORG)}\right]} \qquad (4.5)$$
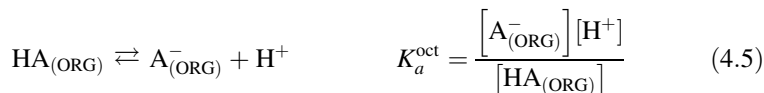
Characteristic of a box diagram, the difference between the partition coefficients is equal to the difference between the two pK_a values [229,275,280,362]:

$$diff\,(\log P^{N-I}) = \log P^N - \log P^I = \left|pK_a^{oct} - pK_a\right| \qquad (4.6)$$

In a box diagram, if any three of the equilibrium constants are known, the fourth may be readily calculated from Eq. (4.6), taking into account that octanol causes the pK_a of weak acids to increase, and that of weak bases to decrease.

In mixtures containing high lipid : water ratios, HCl will appreciably partition into solutions with pH <2.5, as will KOH when pH >11.5 [162,284]. General box diagrams reflecting these caveats have been discussed [275].

4.2   CONDITIONAL CONSTANTS

The constants in Eqs. (4.4) and (4.5) are *conditional* constants. Their value depends on the background salt used in the *constant ionic medium reference state* (Section 3.1). In the partition reactions considered, the ionized species migrating into the oil phase is accompanied by a counterion, forming a charge-neutral ion pair. The lipophilic nature and concentration of the counterion (as well as that of the charged drug) influences the values of the the ion pair constants. This was clearly illustrated [277] in the study of the partitioning of the charged form of chlorpromazine into octanol at pH 3.9 (pK_a 9.24 [150]) in the 0.125 M background salt concentrations: $P^I = 56$ (KBr), 55 (NaPrSO$_3$), 50 (KNO$_3$), 32 (KCl, NaCl), 31 (NH$_4$Cl), 26 (Me$_4$NCl), 25 (NaEtSO$_3$), 19 (Et$_4$NCl), 16 (Pr$_4$NCl), 15 (Na$_2$SO$_4$, NaMeSO$_3$), 13 (KCl + 2M urea), and 5 (no extra salt used), suggesting the counterion lipophilicity scale: Br$^-$ > PrSO$_3^-$ > NO$_3^-$ > Cl$^-$ > EtSO$_3^-$ > SO$_4^{2-}$, MeSO$_3^-$. An additional example along this line was described by van der Giesen and Janssen [279], who observed the relationship $\log P^I = 1.00 \log[\text{Na}^+] + 0.63$ for warfarin at pH 11, as a function of sodium concentration. In all the following discussions addressing ion pairs, it is be assumed that 0.15 M KCl or NaCl is the background salt, unless otherwise indicated.

4.3   log *P* DATABASES

A large list of log *P* values has been tabulated by Leo et al. in a 1971 review [364]. Commercial databases are available [365–369]. The best known is the Pomona College MedChem Database [367], containing 53,000 log *P* values, with 11,000 confirmed to be of high quality, the "log *P*-star" list. (No comparably extensive listing of log *D* values has been reported.) Table 4.1 lists a set of "gold standard" octanol–water $\log P^N, \log P^I$ and $\log D_{7.4}$ values of mostly drug-like molecules, determined by the pH-metric method.

4.4   log *D*

The distribution ratio *D* is used only in the context of ionizable molecules [229,270–276]. Otherwise, *D* and *P* are the same. The partition coefficient *P*, defined in Eq. (4.2), refers to the concentration ratio of a *single* species. In contrast,

the distribution coefficient D can refer to a collection of species and can depend on pH. In the most general sense, D is defined as the sum of the concentrations of all charge-state forms of a substance dissolved in the lipid phase divided by the sum of those dissolved in water. For a simple multiprotic molecule X, the distribution ratio is defined as

$$D = \frac{([X_{(ORG)}]' + [XH_{(ORG)}]' + [XH_{2(ORG)}]' + \cdots)/([X] + [XH] + [XH_2] + \cdots)}{r}$$

(4.7)

where r is the lipid–water volume ratio, $v(ORG)/v(H_2O)$. The primed quantity is defined in concentration units of moles of species dissolved in the organic phase per liter of *aqueous* phase. Assuming a diprotic molecule and substituting Eqs. (3.7), (3.8), (4.2), and (4.4) into Eq. (4.7) yields

$$D = \frac{P_A + P_{HA}10^{+(pK_{a2}-pH)} + P_{H_2A}10^{+(pK_{a2}+pK_{a1}-2\,pH)}}{1 + 10^{+(pK_{a2}-pH)} + 10^{+(pK_{a2}+pK_{a1}-2\,pH)}}$$

(4.8)

where P_A refers to the ion pair partition coefficient of the dianion; P_{HA}, to that of the anion, and P_{H_2A}, to the partition coefficient of the neutral species. If no ion pair partitioning takes place, then Eq. (4.8) further simplifies to

$$\log D = \log P^N - \log\{1 + 10^{-(pK_{a2}+pK_{a1}-2pH)} + 10^{-(pK_{a1}-pH)}\}$$

(4.9)

Note that the distribution coefficient depends only on pH, pK_a values, and P (not on concentration of sample species). Equation (4.7) is applicable to all lipophilicity calculations. Special cases, such as eq. 4.9, have been tabulated [275].

Figures 4.2a, 4.3a, and 4.4a show examples of lipophilicity profiles, $\log D$ versus pH, of an acid (ibuprofen), a base (chlorpromazine), and an ampholyte (morphine). The flat regions in Figs. 4.2a and 4.3a indicate that the $\log D$ values have reached the asymptotic limit where they are equal to $\log P$: at one end, $\log P^N$ and at the other end, $\log P^I$. (The morphine example in Fig. 4.4a is shown free of substantial ion pair partitioning.) The other regions in the curves have the slope of either -1 (Fig. 4.2a) or $+1$ (Fig. 4.3a) or ± 1 (Fig. 4.4a). Ibuprofen has the octanol–water $\log P_{HA}$ 3.97 (indicated by the flat region, pH $<$ 4, Fig. 4.2a) and the ion pair $\log P_A$ -0.05 in 0.15 M KCl (flat region, pH $>$ 7) [161]. Chlorpromazine has $\log P_B$ 5.40 and an ion-pair $\log P_{BH}$ 1.67, also in 0.15 M KCl (Fig. 4.3a) [161]. Ion pairing becomes significant for pH $<$ 6 with the base. The equation that describes the sigmoidal curve, valid for monoprotic acids and bases for the entire pH range, is

$$\log D = \log(P_X + P_{XH}10^{+pK_a-pH}) - \log(1 + 10^{+pK_a-pH})$$

(4.10)

Figure 4.2 (a) Lipophilicity profile of a weak acid at two values of background salt and (b) log–log speciation plot at 0.15 M KCl. [Avdeef, A., *Curr. Topics Med. Chem.*, **1**, 277–351 (2001). Reproduced with permission from Bentham Science Publishers, Ltd.]

For a weak acid, $P_{XH} > P_X$ and the log D curve decreases with pH; for a weak base, $P_X > P_{XH}$, and the log D curve increases with pH, according to this equation.

An additional and useful property of lipophilicity profiles is that the pK_a values are indicated at points where the horizontal asymptote lines intersect the diagonal lines (where $d \log D / d\,pH = 0.5$ [275]). In Fig. 4.2a, the pK_a and pK_a^{oct} (see Fig. 4.1)
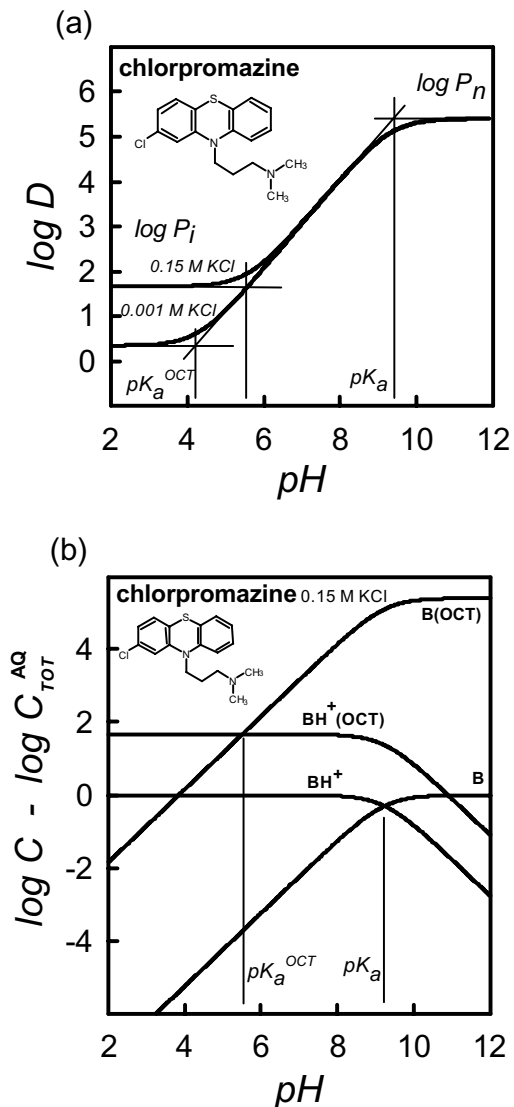
Figure 4.3 (a) Lipophilicity profile of a weak base at two values of background salt and (b) log–log speciation plot at 0.15 M KCl. [Avdeef, A., *Curr. Topics Med. Chem.*, **1**, 277–351 (2001). Reproduced with permission from Bentham Science Publishers, Ltd.]

values are 4.45 and 8.47, respectively; in Fig. 4.3a, the two values are 9.24 and 5.51, respectively. Since pK_a^{oct} is associated with ion pairing, its value depends on the ionic strength, as discussed above. This is clearly evident in Figs. 4.2a and 4.3a.

It may surprise some that for a diprotic molecule with overlapping pK_a values the region of maximum log D (0.76 in Fig. 4.4a) does *not* equal log P; a displaced horizontal line in Fig. 4.4a indicates the log P to be 0.89 for morphine [161,162].
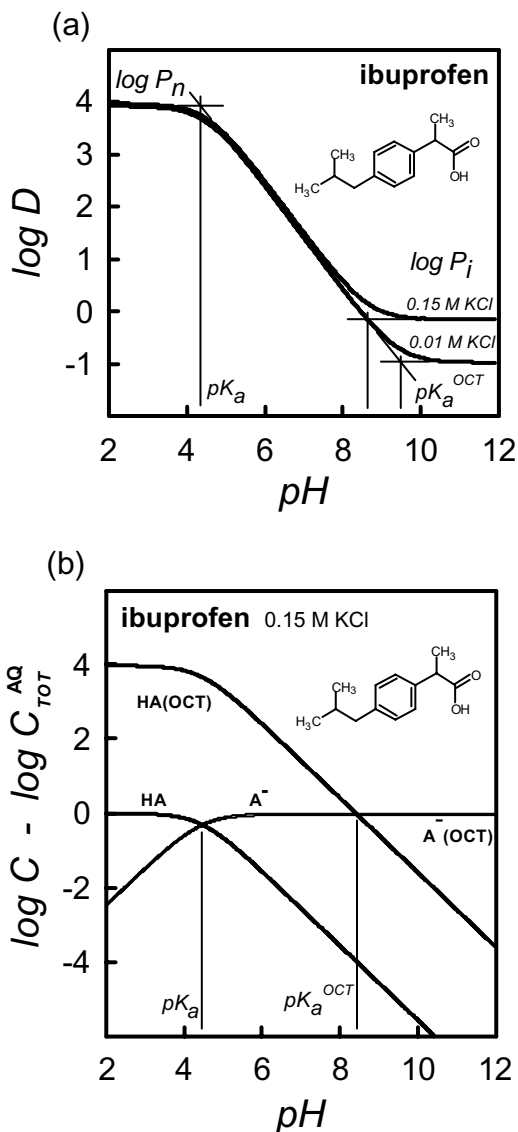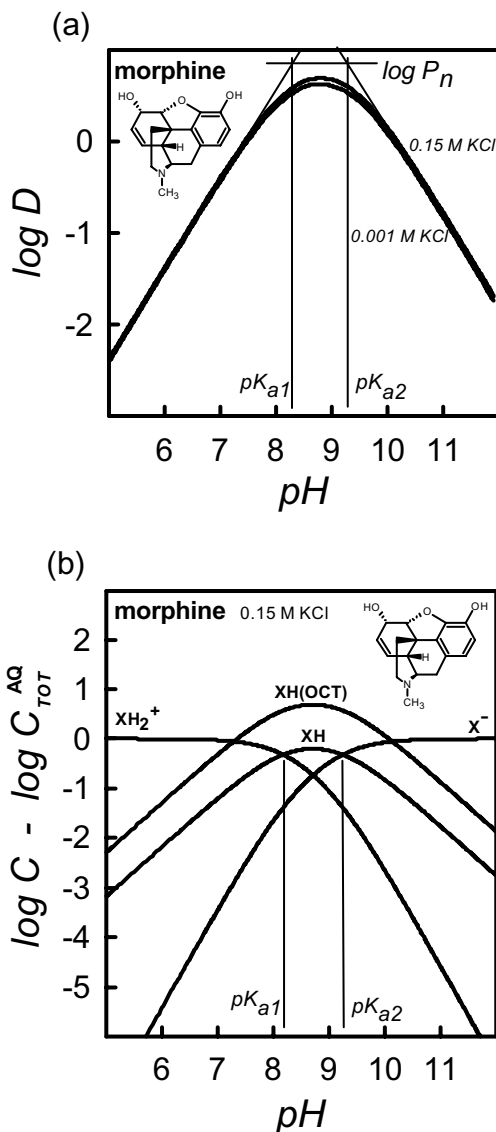
Figure 4.4 (a) Lipophilicity profile of an ampholyte at two values of background salt and (b) log–log speciation plot at 0.15 M KCl. [Avdeef, A., *Curr. Topics Med. Chem.*, **1**, 277–351 (2001). Reproduced with permission from Bentham Science Publishers, Ltd.]

Figures 4.2b, 4.3b, and 4.4b are log–log speciation plots, indicating the concentrations of species in units of the total aqueous sample concentration. (Similar plots were described by Scherrer [280].) The uppermost curve in Fig. 4.2b shows the concentration of the uncharged species in octanol, as a function of pH. If only uncharged species permeate across lipid membranes, as the pH-partition hypothesis

suggests, then this curve deserves attention, perhaps more so than the $\log D$ curve (unless the active site is in the apical membrane outer leaflet of the epithelial cell surface, where permeation of the membrane by the charged species is not necessary). That curve is like that of the $\log D$ curve, but with the ion-pair component removed.

4.5   PARTITIONING OF QUATERNARY AMMONIUM DRUGS

The octanol–water partitioning behavior of orally active quaternary ammonium drugs (which are always charged in the physiological pH range), such as propantheline, trantheline, homidium, and neostigmine, was reported by Takács-Novák and Szász [291]. Propanetheline has 10% oral absorption, whereas neostigmine is very poorly absorbed from the GIT [370]. Consistent with this, the octanol–water $\log P$ of the bromide salts range from -1.1 to <-3 [291]. However, in the presence of a 50-fold excess of the bile salt deoxycholate, the homidium apparent partition coefficient, $\log P$, elevates to $+2.18$. Similarly heightened numbers were seen when the quaternary drugs were combined with prostaglandin anions, suggesting a possible role of endogenous lipophilic counterions in the GI absorption of the quaternary ammonium drugs.

4.6   log *D* OF MULTIPROTIC DRUGS AND THE COMMON-ION EFFECT

Ion pair partitioning effects with simple salts should no longer be surprising, given the examples presented above. Partitioning of multiprotic molecules, however, warrants additional consideration. The partitioning behavior of charged molecules, including zwitterions (peptide and other kinds) and ordinary ampholytes, has been intriguing [229,276,278,282,283,285–289,371]. These molecules are sometimes charged over the physiological pH range. Scherrer proposed a classification system for ampholytes based on their pK_a–pK_a^{oct} relationships [276]. It is an important topic to understand, since the oral absorption of such molecules can be poor, and methods to overcome it are the focus of many efforts.

   When the $\log D$/pH measurement of a peptide is performed by the shake-flask or the partition chromatography method (using hydrophilic buffers to control pH), usually the shape of the curve is that of a *parabola* (see Ref. 371 and Fig. 1 in Ref. 282), where the maximum $\log D$ value corresponds to the pH at the isoelectric point (near pH 5–6). Surprisingly, when the potentiometric method is used to characterize the same peptide [275], the curve produced is a *step function*, as indicated by the thick line in Fig. 4.5 for dipeptide Trp-Phe.

   Both results (parabola vs. step) are correct, even though there is a big difference in the profiles. The explanation for the difference lies in charged-species partitioning: the counterion (from background salt *or buffer*) plays an ineluctable role. In the potentiometric method, pH is controlled by adding HCl or KOH, to a solution that has a 0.15 M physiological level of salt (KCl or NaCl). Thus, the partitioning
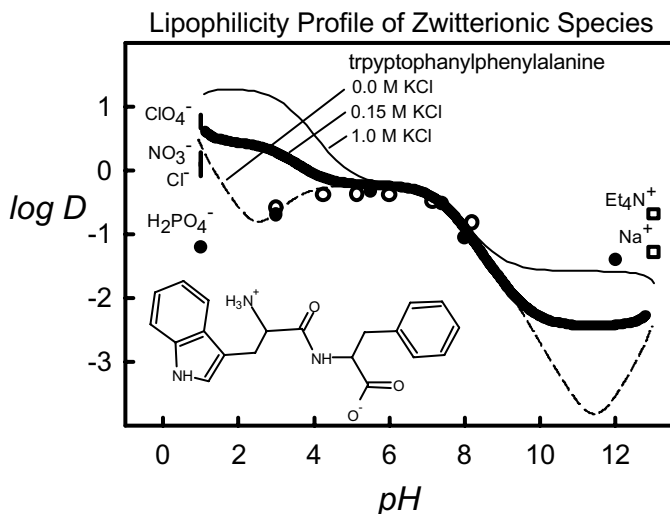
Figure 4.5 Potentiometrically determined [162] lipophilicity profiles of a dipeptide, showing the effect of background salt concentrations. The unfilled symbols [282] and the filled symbols [371] are based on shake-flask measurements. [Avdeef, A., *Curr. Topics Med. Chem.*, **1**, 277–351 (2001). Reproduced with permission from Bentham Science Publishers, Ltd.]

medium always has at least 0.15 M K$^+$ and Cl$^-$ with which to associate into ion pairs. The effect of buffers in shake-flask or HPLC assays is not always taken into account in discussions of results. We can see in Figs. 4.2a and 4.3a, that the log *D* profiles take on different values when the background salt is reduced from 0.15 to 0.001–0.01 M. In Fig. 4.5, we indicate what happens to the log *D* curve when three different levels of salt are used. Very good match to the ''anomalous'' values, indicated by open and closed symbols, is found [282,371]. The upward turns in the dashed curve in Fig. 4.5 for pH >11.5 and <2.5 are due to the common-ion effect of the salt introduced by the titrant: K$^+$ (from KOH) and Cl$^-$ (from HCl), respectively.

In studies of the salt dependence of peptides, an attempt was made to look for evidence of ion triplet formation [162], as suggested by the work of Tomlinson and Davis [278]. Phe-Phe-Phe was used as a test tripeptide, and it was reasoned that by performing the octanol–water partitioning in an aqueous solution containing different levels of salt (0.02–0.50 M KCl), one might see the zwitterion log *P* show the salt dependence that is to be expected of an ion triplet formation. None was evident (other than for the cation at low pH and the anion at high pH, as expected of simple ion-extraction reactions) [162]. An interesting explanation was suggested Dr. Miloň Tichý [1995, unpublished], based on conformational analysis of the structure of the tripeptide in water, that Phe-Phe-Phe can form a cyclic structure, with an intramolecular (internally-compensated) electrostatic bond, ($-CO_2^- \cdots {}^+NH_3-$), formed between the two ends of the molecule. A highly stabilized ring structure may be more stable than a K$^+ \cdots {}^-O_2C$)—($NH_3^+ \cdots Cl^-$ ion triplet.
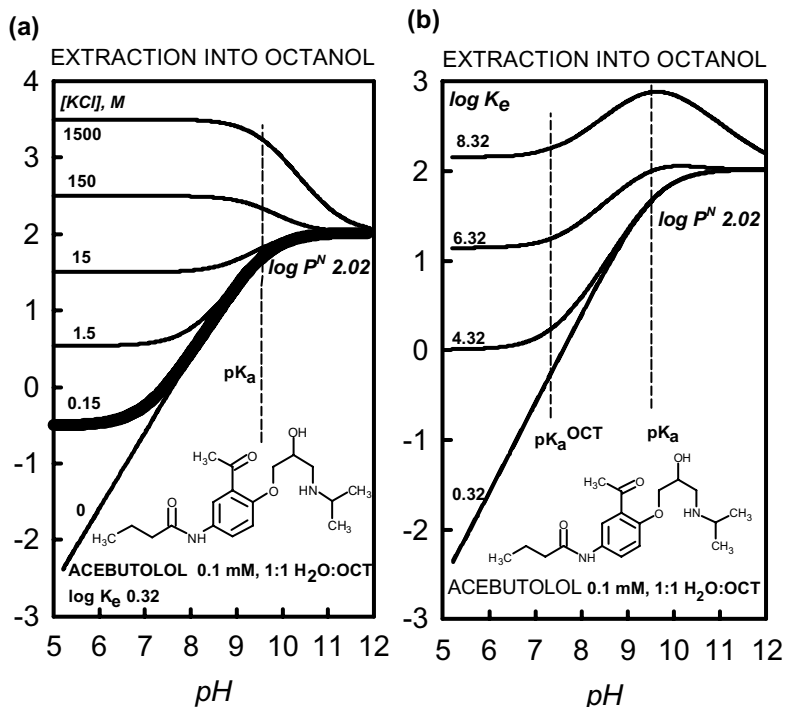
Figure 4.6 Hypothetical lipophilicity profiles: (a) fixed extraction constant with differing salt concentrations; (b) fixed salt concentration with differing extraction constants. [Avdeef, A., *Curr. Topics Med. Chem.*, **1**, 277–351 (2001). Reproduced with permission from Bentham Science Publishers, Ltd.]

The next example, shown in Fig. 4.6a, is the amusing consequence of continually increasing the concentration of background salt (beyond its aqueous solubility—just to make the point) to the shape of $\log D$/pH profile for acebutolol (whose normal 0.15 M salt curve [362] is indicated by the thick line in Fig. 4.6a). The base-like (cf. Fig. 4.3a) lipophilicity curve shape at low levels of salt can become an acid-like shape (cf. Fig. 4.2a) at high levels of salt! An actual example of a dramatic reversal of character is the ionophore monensin, which has a $\log P^I$ (in a background of Na^+) 0.5 *greater* than $\log P^N$ [276,281].

To cap off the topic of salt dependence, is the following example (also using acebutolol), which will indeed surprise most readers, at first. It is possible to have a peak in a $\log D$/pH profile of a monoprotic molecule! In Fig. 4.6b, we simulated the case by assuming that the level of salt was kept constant and *equal* to the concentration of the sample, and proceeded to explore what should happen if the log of the extraction constant K_e [162,225,275,277]

$$BH^+ + Cl^- \rightleftarrows BH^+Cl^-_{(ORG)} \qquad K_e = \frac{[BH^+Cl^-_{(ORG)}]}{[BH^+][Cl^-]} \qquad (4.11)$$

were raised from the value 0.32 [362] to higher values. The $\log D$ profile eventually develops a peak at $pH = pK_a$ and the series of curves in Fig. 4.6b all have the same pK_a^{oct}, whose value is equal to $pK_a - \log P^N$, namely, 7.5 [Eq. (4.10) is inadequate to explain the phenomenon]. Similarly shaped curves were reported by Krämer et al. [368], who considered the partitioning of propranolol into liposomes (containing free fatty acids) that had *surface charge* that was pH-dependent. In the present case of salt-induced extraction, the maximum point in Fig. 4.6b is not sustainable as pH increases past the pK_a, because the concentration of the charged sample component diminishes, in accordance with the pK_a.

4.7 SUMMARY OF CHARGED-SPECIES PARTITIONING IN OCTANOL–WATER

Excluding effects not in the scope of this book, such as interfacial transport of charged species driven by electrical potentials, the main lesson of the partitioning studies of charged drugs is that the charged molecule needs to be accompanied by a counterion in order for the ion pair to enter a lipid phase such as octanol. Later, it will become apparent that it must not be taken for granted that charged species enter other lipid phases as they do octanol. The peculiar structure of octanol (Fig. 2.8) may facilitate the entry of ion pairs in a way that may be impossible in a phospholipid bilayer, for example (covered below).

Scherrer observed [280,281], as have others [161,162,275], that for a large number of ordinary charged species partitioning into octanol in the presence of aqueous solutions containing 0.15 M KCl or NaCl, weak-acid salts have values of $diff(\log P^{N-I})$ equal to $\sim$4, and that weak-base salts have *diff* values equal to $\sim$3. These are helpful numbers to keep in mind when predicting the values of $\log P^I$ when $\log P^N$ is known.

Scherrer identified the conditions where *diff* 3–4 may be transgressed: (1) if the drug has several polar groups or a large polar surface over which charge can be delocalized, then smaller values of *diff* are observed; (2) hydroxyl groups adjacent to amines or carboxylic groups stabilize ion pairs, leading to lower *diff* values; and (3) steric hindrance to solvation leads to higher values of *diff*, as seen with tertiary amines, compared to primary ones [280,281].

4.8 ION PAIR ABSORPTION OF IONIZED DRUGS— FACT OR FICTION?

A review article with this title appeared in 1983 [369]. It's an old question, one not fully resolved: What does the charged-species partitioning seen in octanol–water systems have to do with biological systems? If getting to the receptor site involves passing through many lipid membranes, and if the pH partition hypothesis is to hold, the answer to the question is a resounding "Nothing." If the active site is in the outer leaflet of the apical membrane and the drug is orally introduced, or

if ocular or skin absorption is considered [372,373], the answer is "Maybe something." We will return to this question in several instances in the next sections, for its answer warrants serious consideration.

4.9   MICRO-log P

We considered micro-pK_a values in Section 3.6. A parallel concept applies to partition coefficients (of multiprotic molecules); namely, if an ionizable substance of a particular stoichiometric composition can exist in different structural forms, then it is possible for each form to have a different micro-log P [224,243,273,275]. When log P is determined by the potentiometric method (below), the constant determined is the macro-log P. Other log P methods may also determine only the macroscopic constant.

Niflumic acid, which has two pK_a values, was studied both pH-metrically and spectroscopically using the shake-flask method [224]. The monoprotonated species can exist in two forms: (1) zwitterion, $XH^{\pm}$ and (2) ordinary (uncharged) ampholyte, XH^0. The ratio between the two forms (tautomeric ratio) was measured spectroscopically to be 17.4. On assuming that a negligible amount of zwitterion $XH^{\pm}$ partitions into octanol, the calculated micro-log P for XH^0 was 5.1, quite a bit higher than the macro-log P 3.9 determined pH-metrically in 0.15 M NaCl. It is noteworthy that the distribution coefficient D is the same regardless of whether the species are described with microconstants or macroconstants [275].

4.10   HPLC METHODS

HPLC log P techniques, first described by Mirrlees et al. [374] and Unger et al., [375], are probably the most frequently used methods for determining log P. The directly measured retention parameters are hydrophobicity indices, and need to be converted to a log P scale through the use of standards. The newest variants, breadths of scope, and limitations have been described in the literature [292–298]. A commercial automated HPLC system based on an extension of the approach described by Slater et al. [150] has just introduced by Sirius (`www.sirius-analytical.com`).

4.11   IAM CHROMATOGRAPHY

A very promising method, immobilized artificial membrane (IAM) chromatography, was developed by Pidgeon and co-workers [299–304,307], where silica resin was modified by covalent attachment of phospholipid-like groups to the surface. The retention parameters mimic the partitioning of drugs into phospholipid bilayers. The topic has been widely reviewed [47,298,307,309–311].

4.12   LIPOSOME CHROMATOGRAPHY

A method where phospholipids are entrapped in the pores of resin beads, in the forms of multilamellar vesicles, has been described [313–319,376]. In some ways, the idea is similar to that of IAM chromatography, even though the resin is modified differently. The retention indices correlate very well with the partition coefficients measured in liposome–water systems (described below).

4.13   OTHER CHROMATOGRAPHIC METHODS

Capillary electrophoresis (CE) (see Section 3.5) has been used to determine partition coefficients [320–322]. Lipid vesicles or micelles are added to the buffer whose pH is adjusted to different values. Since drug molecules partition to a different extent as a function of pH, the analysis of mobility vs pH data yields log P values.

   Centrifugal partition chromatography (CPC) has been used to characterize the partitioning behavior of hydrophilic molecules, where log D values as low as -3 can be obtained [371,377–379]. It is not as popular a method as it used to be, apparently due to instrumental challenges. Cyclic voltammetry (CV) has become the new method used to get access to very low log D values, with partition coefficients reported as low as -9.8 [261,269,362].

4.14   pH–METRIC log P METHOD

In 1952, Dyrssen (using a radiometer titrator) performed the first dual-phase titrations to determine oil–water partition coefficients [324]. In a series of papers on solvent extraction of metal complexes, he and co-workers [324–331] measured neutral and ion pair log P of compounds, studied dimerization reactions of dialkylphosphates in aqueous as well as chloroform solutions, used log D/pH plots, and derived a method for deducing the pK_a of water-insoluble molecules from knowledge of their log P, later called the *PDP* method [112]. In 1963, Brändström [332], using a pH-stat titrator, applied the log P methods to pharmaceutical problems. In the mid-1970s, the technique was "reborn." Seiler described a method where the pK_a and log P were determined simultaneously from a single titration [250]. At about the same time, working independently, Koreman and Gur'ev [333], Kaufman et al. [334], and Johansson and Gustavii [335,336] published in this area. Gur'ev and co-workers continued to apply the method, but their work was not well known outside of Russian literature [337–343]. Clarke and others [344,345,350,351] presented a comprehensive treatment of the technique, and applied it to mono-, di- and triprotic substances. Numerical differentiation and matrix algebra were used to solve a number of simultaneous equations. Both graphical and refinement procedures for dealing with ion pair formation were devised. A dual-phase microtitration system has been described [361]. The rigorous development of the

pH-metric method continued in a commercial setting by Avdeef and colleagues [25,112,149–151,153,161,162,224,225,275,346–349,352,357,362].

The pH-metric technique consists of two linked titrations. Typically, a pre-acidified 100–500 µM solution of a weak acid is titrated with standardized 0.5 M KOH to some appropriately high pH; octanol (or any other useful organic partition solvent that is immiscible with water) is then added (in low relative amounts for lipophilic molecules and high amounts for hydrophilic molecules), and the dual-solvent mixture is titrated with standardized 0.5 M HCl back to the starting pH. After each titrant addition, pH is measured. If the weak acid partitions into the octanol phase, the two assays show nonoverlapping titration curves. The greatest divergence between the two curves occurs in the buffer region. Since the pK_a is approximately equal to the pH at the midbuffer inflection point, the two-part assay yields two constants: pK_a and p_oK_a, where p_oK_a is the apparent constant derived from the octanol-containing segment of data. A large difference between pK_a and p_oK_a indicates a large value of $\log P$.

Bjerrum analysis (Section 3.3.1) is used for initial processing of the titration data. Figure 4.7a shows the Bjerrum plots of the two segments of the titration of a weak acid, phenobarbital [150]. The solid curve corresponds to the octanol-free segment, and the dotted curve corresponds to the curve obtained from the octanol-containing data, where r, the octanol–water volume ratio, is 1 in the example. As said before (Sec. 3.3.1), the pK_a and p_oK_a may be read off the curve at half-integral values of $\bar{n}_H$. From the difference between pK_a and p_oK_a, one obtains [347]

$$P_{HA} = \frac{10^{+(p_oK_a - pK_a)} - 1}{r} \tag{4.12}$$

Figure 4.7b shows an example of a weak base, diacetylmorphine (heroin) [151]. The partition coefficient for the weak base is derived from

$$P_B = \frac{10^{-(p_oK_a - pK_a)} - 1}{r} \tag{4.13}$$

If the two phases are equal in volume (1 : 1) and the substance is lipophilic, a very simple relationship can be applied to determine $\log P$;

$$\log P_{HA} \approx (p_oK_a^{1:1} - pK_a) \qquad (\log P_B \approx -(p_oK_a^{1:1} - pK_a)) \tag{4.14}$$

Note that for a weak acid, the octanol causes the Bjerrum curve to shift in the direction of higher pH, whereas for a weak base, octanol causes the shift to lower values of pH. Equation (4.14) may be applied to the molecules in Fig. 4.7, and $\log P$ deduced from the shifts in the curves.

For diprotic molecules, 12 different characteristic shift patterns have been identified for cases where two species may partition simultaneously into the lipid phase [347]. Three of these cases are shown in Fig. 4.8, picking familiar drug substances as examples. Once the approximate constants are obtained from Bjerrum analysis,

(a)

(b)
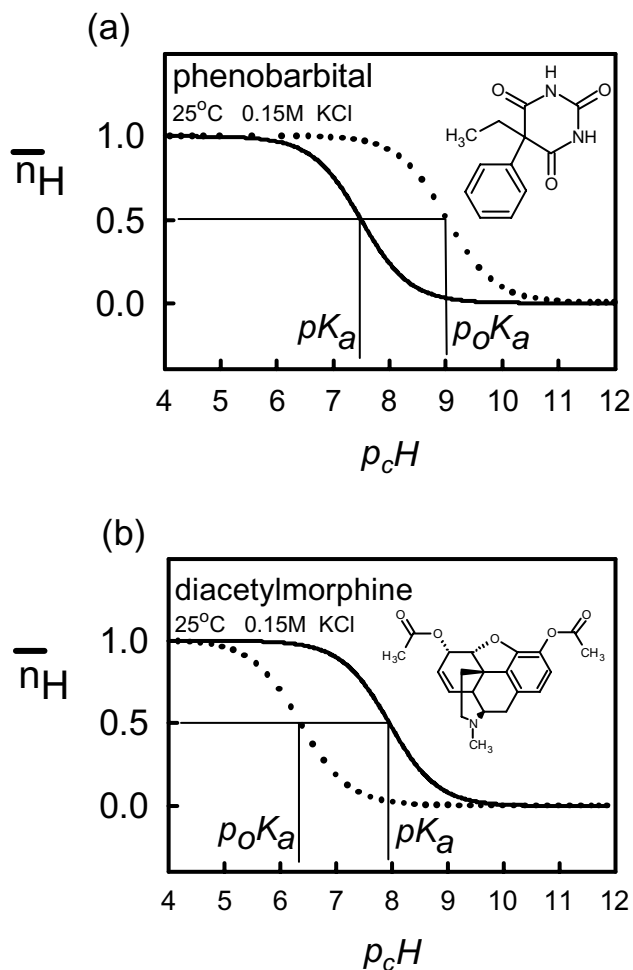
Figure 4.7   Octanol–water Bjerrum plots for a monoprotic (a) acid and (b) base. The volumes of octanol and water are equal, so that the difference between the apparent pK_a and the true pK_a is about equal to the partition coefficient. [Avdeef, A., *Curr. Topics Med. Chem.*, **1**, 277–351 (2001). Reproduced with permission from Bentham Science Publishers, Ltd.]

they may be further refined by a weighted [117] nonlinear least-squares procedure [153].

The pH-metric procedure has been validated against the standard shake-flask method [150,357], and many studies using it have been reported [56,149–151,153,161,162,224,225,229,246,250,268,269,275,276,280,281,324–363]. Determinations of values of log P as low as −2 and as high as +8 have been documented [161,162,352]. The published literature clearly indicates that the Dyrssen technique is a reliable, versatile, dynamic, and accurate method for measuring log P. It may lack the speed of HPLC methods, and it cannot go as low in log P as the CV
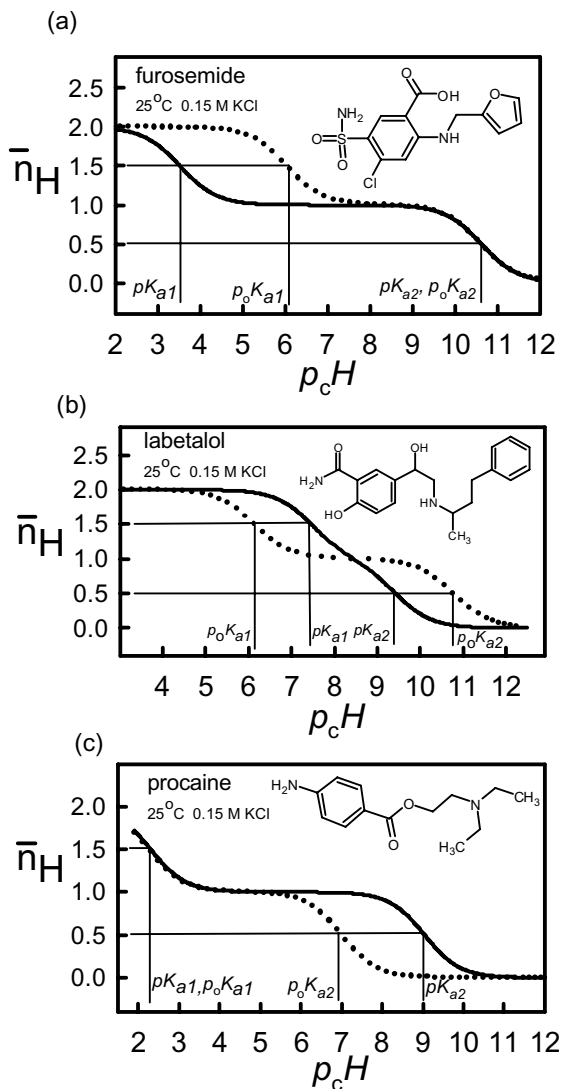
Figure 4.8   Octanol–water Bjerrum plots for a diprotic (a) acid, (b) ampholyte, and (c) base. The volumes of octanol and water are equal, so that the difference between the apparent pK_a and the true pK_a is about equal to the partition coefficient. [Avdeef, A., *Curr. Topics Med. Chem.*, **1**, 277–351 (2001). Reproduced with permission from Bentham Science Publishers, Ltd.]

method, but all in all, it is well positioned to replace the shake-flask procedure as the primary validation method for ionizable molecules. What keeps it from being the "gold standard," its Achilles' heel, is that the sample molecules must be ionizable and have a pK_a in the measurable pH range.

4.15 HIGH-THROUGHPUT $\log P$ METHODS

Several efforts have been made to increase the throughput of the traditional $\log P$ methods by scaling down to a 96–well microtiter plate format [294]. The generic fast gradient HPLC methods look promising (see Section 4.10). The commercial HPLC system (see Section 4.10) shows promise of industrywide standardization. Immobilized liposome and IAM chromatography methods can also be fast (see Sections 4.11 and 4.12) All the chromatography methods suffer from being essentially series-based assays.

Parallel methods using scanning 96/384-well plate UV spectrophotometers are inherently faster [292]. They will become 50-fold faster with the imminent introduction of diode-array plate readers.

4.16 OCTANOL–WATER $\log P^N$, $\log P^I$, AND $\log D_{7.4}$ "GOLD STANDARD" FOR DRUG MOLECULES

About 300 values of octanol–water $\log P^N$, $\log P^I$, and $\log D_{7.4}$ of drugs and some agrochemicals are listed in Table 4.1. These have been critically selected to represent high-quality results. Most of these constants have been determined at Sirius or pION since 1991, with many personally determined by the author.

TABLE 4.1 Critically Selected Experimental $\log P^N$, $\log P^I$, and $\log D_{7.4}$ of Drug Molecules[a]

Compound	$\log P^N$	$\log P^I(+)$	$\log P^I(-)$	$\log D_{7.4}$	Ref.
1-Benzylimidazole	1.60	—	—	—	112, p. 70
2,4-Dichlorophenoxyacetic acid	2.78	—	−0.87	−0.82	161, p. 63
2-Aminobenzoic acid	1.26	—	—	−1.31	161, p. 8
3,4-Dichlorophenol	3.39	—	—	—	150
3,5-Dichlorophenol	3.63	—	—	3.56	150
3-Aminobenzoic acid	0.34	−0.93	—	−2.38	161, p. 25
3-Bromoquinoline	2.91	—	—	2.91	150
3-Chlorophenol	2.57	—	—	2.56	150
4-Aminobenzoic acid	0.86	−0.40	—	−1.77	161, p. 105
4-Butoxyphenol	2.87	—	—	—	150
4-Chlorophenol	2.45	—	—	—	150
4-Ethoxyphenol	1.81	—	—	—	150
4-Iodophenol	2.90	—	—	—	150
4-Methoxyphenol	1.41	—	—	—	150
4-Methylumbilleferyl-β-D-glucuronide	−0.39	—	—	—	151

TABLE 4.1   (*Continued*)

Compound	log P^N	log $P^I(+)$	log $P^I(-)$	log $D_{7.4}$	Ref.
4-Pentoxyphenol	3.26	—	—	—	150
4-Phenylbutylamine	2.39	−0.45	—	−0.62	149
4-Propoxyphenol	2.31	—	—	—	150
5-Phenylvaleric acid	2.92	—	−0.95	1.69	149
6-Acetylmorphine	1.55	−0.42	—	0.61	151
Acebutolol	2.02	−0.50	—	−0.09	362
Acetaminophen	0.34	—	—	0.34	357
Acetic acid	−0.30	—	—	−2.88	—[c]
Acetophenone	1.58	—	—	1.58	296
Acetylsalicylic acid	0.90	—	—	−2.25	161, p. 167
Alprazolam	2.61	—	—	2.08	550
Alprenolol	2.99	0.21	—	0.86	362
Aminopyrine (aminophenazone)	0.85	—	—	0.63	357
Amiodarone	7.80	4.02	—	6.10	—[b]
Amitriptyline	4.62	0.16	—	2.80	—[b]
Amitrole	−0.97	—	—	—	265
Amlodipine	3.74	1.09	—	2.25	—[c]
Amoxicillin	−1.71	−1.22	−1.56	−2.56	56
Ampicillin	−2.17	−1.15	−1.31	−1.85	162, p. 133
Amylobarbitone	2.01	—	—	—	150
Antipyrine (phenazone)	0.56	—	—	0.56	56
Ascorbic acid	−1.85	—	—	−4.82	357
Atenolol	0.22	—	—	−2.01	362
Atropine	1.89	−1.99	—	−0.66	—[b]
Azithromycin	3.87	0.23	—	0.33	—[b]
Bentazone	2.83	—	—	—	265
Benzocaine	1.89	—	—	1.90	162, p. 25
Benzoic acid	1.96	—	—	−1.25	150
Betamethasone	2.06	—	—	2.10	550
Bifonazole	4.77	—	—	4.77	296
Bisoprolol	2.15	−1.22	—	—	362
Bromazepam	1.65	—	—	1.65	296
Bromocriptine	4.20	—	—	4.20	509
Bumetanide	4.06	—	—	−0.11	561
Buprenorphine	4.82	0.09	—	3.75	151
Bupropion	3.21	—	—	2.61	561
Buspirone	2.78	—	—	—	357
Butobarbitone	1.58	—	—	—	150
Caffeine	−0.07	—	—	−0.07	296
Captopril	1.02	—	—	−2.00	561
Carazolol	3.73	0.77	—	1.58	362
Carbamazepine	2.45	—	—	2.45	56
Carbomycin A	3.04	—	—	—	358
Carbomycin B	3.52	—	—	—	358

TABLE 4.1 (*Continued*)

Compound	log P^N	log P^I (+)	log P^I (−)	log $D_{7.4}$	Ref.
Carvedilol	4.14	1.95	—	3.53	362
Cefadroxil	−0.09	—	—	−1.77	561
Cefalexin	0.65	—	—	−1.00	561
Cefixime	0.11	—	—	−0.79	550
Cefoxitin	1.55	—	—	−0.60	550
Celiprolol	1.92	—	—	−0.16	150
Chlorambucil	3.70	—	—	0.61	550
Chloramphenicol	1.14	—	—	1.14	296
Chloroquine	4.69	—	—	0.89	550
Chlorothiazide	−0.24	—	—	−0.05	561
Chlorpheniramine	3.39	—	—	1.41	296
Chlorpromazine	5.40	1.67	—	3.45	161, p. 163
Chlorprothixene	6.03	—	—	3.71	550
Chlorsulfuron	1.79	—	—	—	265
Chlortalidone	−0.74	—	—	0.78	550
Cimetidine	0.48	—	—	0.34	—[b]
Ciprofloxacin	−1.08	−1.69	—	−1.12	—[b]
Citric acid	−1.64	—	—	—	161, p. 168
Clarithromycin	3.16	—	—	—	358
Clofibrate	3.65	—	—	3.39	561
Clonazepam	3.02	—	—	2.45	550
Clonidine	1.57	—	—	0.62	296
Clopyralid	1.07	—	—	−2.95	265
Clotrimazole	5.20	—	—	5.20	296
Clozapine	4.10	—	—	3.13	509
Cocaine	3.01	—	—	1.07	550
Codeine	1.19	—	—	0.22	151
Coumarin	1.39	—	—	1.44	550
Cromolyn	1.95	—	—	-1.15	561
Dapsone	0.94	—	—	0.68	550
Debrisoquine	0.85	−0.87	—	−0.87	161, p. 119
Deprenyl	2.90	−0.95	—	2.49	162, p. 26
Desipramine	3.79	0.34	—	1.38	—[b]
Desmycarosyl carbomycin A	0.30	—	—	—	358
Desmycosin	1.00	—	—	—	358
Diacetylmorphine	1.59	—	—	—	151
Diclofenac	4.51	—	0.68	1.30	162, p. 146
Diethylstilbestrol	5.07	—	—	5.07	296
Diflunisal	4.32	—	—	0.37	550
Diltiazem	2.89	—	—	2.16	—[b]
Diphenhydramine	3.18	−0.52	—	1.39	—[b]
Disopyramide	2.37	—	—	−0.66	—[b]
Doxorubicin	0.65	—	—	−0.33	550
Doxycycline	0.42	0.09	−0.34	0.23	—[b]
Enalaprilmaleate	0.16	−0.10	—	−1.75	—[b]

TABLE 4.1   (*Continued*)

Compound	$\log P^N$	$\log P^I(+)$	$\log P^I(-)$	$\log D_{7.4}$	Ref.
Enalaprilat	−0.13	−0.99	−1.07	−2.74	56
Ephedrine	1.13	−0.96	—	−0.77	162, p. 131
Ergonovine	1.67	−0.51	—	1.54	—[b]
Erythromycin	2.54	−0.43	—	1.14	—[b]
Erythromycylamine	3.00	—	—	—	358
Erythromycylamine-11,12-carbonate	2.92	—	—	—	358
Ethinylestradiol,17-α	3.42	—	1.29	3.42	—[b]
Ethirimol	2.22	—	—	—	265
Etofylline	−0.49	—	—	−0.27	550
Etoposide	1.97	—	—	1.82	561
Famotidine	−0.81	−0.54	—	−0.62	—[b]
Fenpropimorph	4.93	—	—	—	265
Flamprop	3.09	—	—	—	265
Fluazifop	3.18	—	—	—	265
Fluconazole	0.50	—	—	0.50	296
Flufenamic acid	5.56	—	1.77	2.45	—[b]
Flumazenil	1.64	—	—	1.21	561
Flumequine	1.72	—	—	0.65	161, p. 19
Fluocortolone	2.06	—	—	2.10	550
Flurbiprofen	3.99	—	—	0.91	—[b]
Fluvastatin	4.17	—	1.12	1.14	56
Fomesafen	3.00	—	—	—	265
Furosemide	2.56	—	—	−0.24	—[b]
Gabapentin	−1.25	—	—	−2.00	561
Griseofulvin	2.18	—	—	2.18	296
Guanabenz	3.02	—	—	1.40	561
Haloperidol	3.67	1.32	—	3.18	—[b]
Heptastigmine	4.82	—	—	0.17	550
Homidium bromide	−1.10	—	—	−1.10	291
Hydrochlorothiazide	−0.03	—	−1.59	−0.18	—[b]
Hydrocortisone-21-acetate	2.19	—	—	2.19	296
Hydroflumethiazide	0.54	—	—	0.31	550
Hydroxyzine	3.55	0.99	—	3.13	161, p. 146
Ibuprofen	4.13	—	−0.15	1.44	149
Imazapyr	0.22	—	—	—	265
Imazaquin	1.86	—	—	—	265
Imidacloprid	0.33	—	—	0.33	265
Imipramine	4.39	0.47	—	2.17	—[b]
Indomethacin	3.51	—	−2.00	0.68	—[b]
Ioxynil	3.43	—	—	—	265
Ketoconazole	4.34	—	—	3.83	561
Ketoprofen	3.16	—	-0.95	−0.11	—[b]
Ketorolac	1.265	—	—	−0.27	561
Labetalol	1.33	—	—	1.08	—[b]

TABLE 4.1   (*Continued*)

Compound	log P^N	log P^I(+)	log P^I(−)	log $D_{7.4}$	Ref.
Lasinavir	3.30	—	—	—	509
Leucine	−1.55	−1.58	−2.07	−1.77	56
Lidocaine	2.44	−0.52	—	1.72	149
Lorazepam	2.48	—	—	2.39	550
Lormetazepam	2.72	—	—	2.72	296
Maleic hydrazide	−0.56	—	—	—	265
Mebendazole	2.42	—	—	3.28	550
Mecoprop	3.21	—	—	—	265
Mefluidide	2.02	—	—	—	265
Meloxicam	3.43	−0.03	—	0.12	162, p. 112
Melphalan	−0.52	—	—	−2.00	561
Metergoline	4.75	—	—	3.50	550
Methotrexate	0.54	—	−0.92	−2.93	—[b]
Methylprednisolone	2.10	—	—	2.10	561
Methylthioinosine	0.09	—	—	0.09	296
Methysergide	1.95	—	—	2.13	550
Metipranolol	2.81	−0.26	—	0.55	362
Metoclopramide	2.34	—	—	0.41	550
Metolazone	4.10	—	—	4.10	509
Metoprolol	1.95	−1.10	—	−0.24	362
Metronidazole	−0.02	—	—	−0.02	296
Metsulfuron, methyl-	1.58	—	—	—	265
Morphine sulfate	0.89	−2.05	—	−0.06	151
Morphine-3β-D-glucuronide	−1.10	—	—	−1.12	151
Morphine-6β-D-glucuronide	−0.76	—	—	−0.79	151
Moxonidine	0.90	−0.20	—	—	385
N-Me-deramcylane iodide	−1.12	—	—	−1.12	291
N-Me-quinidine iodide	−1.31	—	—	−1.31	291
Nadolol	0.85	—	—	−1.43	362
Naloxone	2.23	—	—	1.09	550
Naphthalene	3.37	—	—	3.37	296
Naproxen	3.24	—	−0.22	0.09	—[b]
Nicotine	1.32	—	—	0.45	161, p. 36
Nifedipine	3.17	—	—	3.17	296
Niflumic acid	3.88	2.48	0.44	1.43	224
Nifuroxime	1.28	—	—	1.28	296
Nitrazepam	2.38	1.21	0.64	2.38	161, p. 169
Nitrendipine	3.59	—	—	3.50	550
Nitrofurantoin	−0.54	—	—	−0.26	550
Nitrofurazone	0.23	—	—	0.23	296
N-Methylaniline	1.65	—	—	—	150
N-Methyl-D-glucamine	−1.31	—	—	−3.62	225
Norcodeine	0.69	—	—	−1.26	151
Nordiazepam	3.15	—	—	3.01	550
Norfloxacin	1.49	—	—	−0.46	550

TABLE 4.1 (*Continued*)

Compound	$\log P^N$	$\log P^I(+)$	$\log P^I(-)$	$\log D_{7.4}$	Ref.
Normorphine	−0.17	—	—	−1.56	151
Nortriptyline	4.39	1.17	—	1.79	—[b]
Ofloxacin	−0.41	—	−0.84	−0.34	161, p. 9
Oleandomycin	1.69	—	—	—	358
Omeprazole	1.80	—	—	2.15	550
Oxprenolol	2.51	−0.13	—	0.18	362
Papaverine	2.95	−0.22	—	2.89	162, p. 30
Penbutolol	4.62	1.32	—	2.06	362
Penicillin V	2.09	—	—	−0.62	561
Pentachlorophenol	5.12	—	—	—	265
Pentamidine	2.08	—	—	−0.19	550
Pentobarbitone	2.08	—	—	—	150
Pentoxifylline	0.38	—	—	0.33	550
Pericyazine	3.65	—	—	—	150
p-F-Deprenyl	3.06	−0.58	—	2.70	162, p. 28
Phenazopyridine	3.31	1.41	—	3.31	—[b]
Phenobarbital	1.53	—	—	1.51	150
Phenol	1.48	—	—	—	150
Phenylalanine	−1.38	−1.41	—	−1.37	161, p. 116
Phenylbutazone	3.47	—	—	0.47	550
Phenytoin	2.24	—	—	2.17	—[b]
Phe-Phe	−0.63	−0.05	—	−0.98	162, p. 6
Phe-Phe-Phe	0.02	0.82	−0.55	−0.29	162, p. 12
Pilocarpine	0.20	—	—	—	357
Pindolol	1.83	−1.32	—	−0.36	362
Pirimicarb	1.71	—	—	—	265
Pirimiphos, methyl-	3.27	—	—	—	265
Piroxicam	1.98	0.96	−0.38	0.00	162, p. 110
Prazosin	2.16	—	—	1.88	561
Prednisolone	1.69	—	—	1.83	550
Prednisone	1.56	—	—	1.44	550
Primaquine	3.00	1.14	—	1.17	—[b]
Probenecid	3.70	—	−0.52	−0.23	—[b]
Procainamide	1.23	—	—	−0.36	550
Procaine	2.14	−0.81	—	0.43	149
Progesterone	3.48	—	—	3.48	561
Promethazine	4.05	—	—	2.44	—[b]
Propamocarb	1.12	—	—	—	265
Propantheline bromide	−1.07	—	—	−1.07	291
Propoxyphene	4.37	—	—	2.60	—[b]
Propranolol	3.48	0.78	—	1.41	362
Proquazone	3.13	—	—	3.21	550
Prostaglandin E_1	3.20	—	−0.33	0.78	225
Prostaglandin E_2	2.90	—	−0.54	0.41	225
Proxyphylline	−0.14	—	—	−0.07	550

TABLE 4.1   (*Continued*)

Compound	$\log P^N$	$\log P^I(+)$	$\log P^I(-)$	$\log D_{7.4}$	Ref.
Pyridoxine	−0.50	−1.33	—	−0.51	161, p. 19
Pyrimethamine	2.87	—	—	2.44	550
Quinalbarbitone	2.39	—	—	—	150
Quinidine	3.44	—	—	2.41	550
Quinine	3.50	0.88	—	2.19	162, p. 128
Quinmerac	0.78	—	—	—	265
Quinoline	2.15	—	—	2.15	150
Ranitidine	1.28	—	—	−0.53	550
Repromicin	2.49	—	—	—	358
Rifabutine	4.55	2.80	—	—	385
Rifampin	0.49	—	—	0.98	550
Rivastigmine	2.10	—	—	—	509
Rosaramicin	2.19	—	—	—	358
Roxithromycin	3.79	1.02	—	1.92	162, p. 107
Rufinamide	0.90	—	—	—	509
Saccharin	0.91	—	—	−1.00	550
Salicylic acid	2.19	—	—	−1.68	—[c]
Serotonin	0.53	−1.66	—	−2.17	—[c]
Sethoxydim	4.38	—	—	—	265
Sotalol	−0.47	−1.43	—	−1.19	162, p. 167
Sulfadiazine	−0.12	—	—	−0.60	550
Sulfamethazine	0.89	—	—	—	150
Sulfasalazine	3.61	—	0.14	0.08	—[b]
Sulfinpyrazone	2.32	—	—	−0.07	550
Sulfisoxazole	1.01	—	—	−0.56	550
Sulindac	3.60	—	—	0.12	550
Suprofen	2.42	—	—	−0.30	550
Tacrine	3.32	—	—	0.34	550
Tamoxifen	5.26	−2.96	—	4.15	—[b]
Terazosin	2.29	—	—	1.14	561
Terbutaline	−0.08	−1.97	−2.05	−1.35	162, p. 36
Terfenadine	5.52	1.77	—	3.61	—[b]
Tetracaine	3.51	0.22	—	2.29	149
Theophylline	0.00	—	—	0.00	162, p. 128
Thiabendazole	1.94	—	—	1.94	265
Thiamphenicol	−0.27	—	—	−0.27	296
Tilmicosin	3.80	—	—	—	358
Timolol	2.12	−0.94	—	0.03	362
Tolnaftate	5.40	—	—	5.40	296
Tralkoxydim	4.46	—	—	—	265
Tranexamic acid	−1.87	—	—	−3.00	561
Trazodone	1.66	—	—	2.54	296
Triazamate acid	1.62	—	—	—	265
Trimethoprim	0.83	−0.88	—	0.63	—[b]
Trovafloxacin	0.15	−0.65	—	0.07	—[b]

TABLE 4.1 (*Continued*)

Compound	$\log P^N$	$\log P^I(+)$	$\log P^I(-)$	$\log D_{7.4}$	Ref.
Trp-Phe	−0.28	0.33	−2.44	−0.50	162, p. 2
Trp-Trp	−0.10	0.49	−0.99	−0.40	162, p. 8
Tryptophan	−0.77	−0.55	−1.57	−0.77	162, p. 10
Tylosin	1.63	—	—	—	358
Valsartan	3.90	—	—	—	509
Verapamil	4.33	0.71	—	2.51	—[b]
Warfarin	3.54	—	0.04	1.12	149

[a] Measurements at 25°C, 0.15 M ionic strength.
[b]pION.
[c]Sirius Analytical Instruments.